

Superexchange Mediated Charge Hopping in DNA[†]

Joshua Jortner,^{*,‡} M. Bixon,[‡] Alexander A. Voityuk,[§] and Notker Rösch[§]

School of Chemistry, Tel Aviv University, Ramat Aviv, 69978 Tel Aviv, Israel, and Institut für Physikalische und Theoretische Chemie, Technische Universität München, 85747 Garching, Germany

Received: November 15, 2001; In Final Form: February 4, 2002

We explore the relationship between the electronic-nuclear level structure, the electronic couplings, and the dynamics of hole hopping transport in DNA. We utilized the electronic coupling matrix elements for hole transfer between nearest-neighbor nucleobases in DNA [Voityuk, A. A.; Jortner, J.; Bixon, M.; Rösch, N. J. *Chem. Phys.* **2001**, *114*, 5614] to evaluate intrastrand and interstrand superexchange electronic couplings, which determine hole hopping rates within the framework of a semiempirical quantum mechanical-kinetic model. Calculations of the exponential distance (R) dependence of the superexchange mediated intrastrand electronic couplings $|V_{\text{super}}|^2 \propto \exp(-\beta R)$ between guanines (G) in “short” $G^+(T-A)_nG$ ($n \lesssim 3$) duplexes result in $\beta = 0.8\text{--}0.9 \text{ \AA}^{-1}$. We interpret the experimental data on time-resolved hole transport in the presence of a site-specifically bound methyl transferase mutant in DNA [Wagenknecht, H.-A.; Rajsiki, S. R.; Pascally, M.; Stemp, E. D. A.; Barton, J. K. *J. Am. Chem. Soc.* **2001**, *123*, 4400] in terms of composite sequential, interstrand and intrastrand superexchange mediated, and direct interstrand hole hopping. This mechanism accounts for the rate determining step, for the weak duplex size dependence of the rate, and for the long-range charge transport induced by interstrand superexchange via short (T–A) bridges, containing a single mediating nucleobase. For hole transfer via longer (T–A)_{*n*} ($n \gtrsim 3$) bridges, the superexchange mechanism is replaced by the parallel mechanism of thermally induced hole hopping (TIH) via long (A)_{*n*} chains. A kinetic analysis of the experimental data for hole transport through seven GG pairs separated by (T–A)_{*n*} ($n = 2\text{--}5$) bridges across the 3′–5′ strand of the DNA duplex [Sartor, V.; Boone, E.; Schuster, G. B. *J. Phys. Chem. B*, **2001**, *105*, 11057] reveals that the superexchange–TIH crossover occurs at $n = n_c = 3$. The explorations of the range of applicability and the breakdown of the superexchange mechanism in DNA lay the foundations for the scrutiny of the universality and system specificity of this mechanism in large-scale chemical and biophysical systems.

I. Prologue

Wilse Robinson made seminal contributions to modern chemical physics, encompassing pioneering experimental and theoretical explorations of matrix isolation electronic spectroscopy,¹ radiationless transitions,² elementary electronic-vibrational excitations in neat and mixed organic molecular solids,³ and energy transfer in organic molecular crystals.^{4,5} In the latter context of triplet energy transfer in isotopically mixed molecular crystals (e.g., naphthalene and benzene), Nieman and Robinson advanced in 1962 the concept of superexchange mediated triplet energy transfer.^{4,5} They proposed that the triplet impurity band of an isotopically mixed crystal is characterized by superexchange interactions

$$J = \gamma(\gamma/\delta E)^n \quad (1)$$

where γ is the nearest-neighbor impurity-impurity exchange integral and δE represents the energy separation of the impurity excitation from the center of the exciton band, whereas $\gamma/\delta E \ll 1$, as appropriate for a perturbative treatment, and n represents the number of the host molecules separating the two impurities.

The superexchange electronic coupling, eq 1, can be recast as an exponential interimpurity distance (R) dependence

$$J = J_0 \exp(-\bar{\beta}/2R) \quad (2a)$$

where $\bar{\beta} = 2\ln(\delta E/\gamma)/R_0$, $J_0 = \gamma \exp(\bar{\beta}R_0/2)$, and R_0 is the nearest-neighbor distance. The triplet energy transfer rate $k_T = (2\pi/\hbar)|J|^2\rho$, where ρ is the density of final states, is given by

$$k_T = (2\pi J_0^2 \rho/\hbar) \exp(-\bar{\beta}R) \quad (2b)$$

The Robinson superexchange mechanism for triplet energy transfer was extended by Kopelman⁶ for the exploration of the percolation model and by Klafter and Jortner⁷ for the study of Anderson localization of triplet excitations in substitutionally disordered, isotopically mixed molecular crystals.

When Robinson advanced the superexchange mechanism for triplet electronic energy transfer, this mechanism was already of much earlier vintage in other fields, i.e., magnetic interactions in solids and electron transfer (ET) in solution. In 1934 Kramers⁸ studied adiabatic demagnetization in paramagnetic salts, which indicated that small exchange couplings existed even between ions separated by one or several diamagnetic groups. Paramagnetic ions could exert spin-dependent perturbations in the wave functions of intervening diamagnetic ions, thereby transmitting the exchange effect over large distances,⁸ which led to the name “superexchange”.⁹ The concept was revived and extended by

[†] Part of the special issue “G. Wilse Robinson Festschrift”. Dedicated to the memory of G. Wilse Robinson, a tribute to his seminal contributions to science.

* To whom correspondence should be addressed.

[‡] Tel Aviv University.

[§] Technische Universität.

Anderson¹⁰ and applied by McConnell¹¹ to explain magnetic interactions and electron exchange in molecular systems. In 1959, George and Griffith¹² drew attention to the superexchange mechanism in an attempt to interpret electron transfer in bridged metal ion complexes. This stimulated Halpern and Orgel¹³ to calculate the promotion of electron transfer between metal ions by molecular bridges within the framework of superexchange. During the last two decades, the generality and importance of the superexchange mechanism for ET in the condensed phase^{14–19} and in biophysical systems^{19–23} has been widely recognized. The ET rate depends on the details of the electronic structure of the bridge. A necessary condition for the realization of the superexchange in ET pertains to the off-resonance donor-bridge electronic coupling. The role of the bridge electronic structure in a donor (d)–bridge (B_1, B_2, \dots, B_n)–acceptor (a) system can be inferred from the unistep superexchange rate^{19,23}

$$k_{\text{super}} = \frac{2\pi}{\hbar} |V_{\text{super}}|^2 F \quad (3)$$

where F is the (donor–acceptor) nuclear Franck–Condon factor and V_{super} is the electronic coupling

$$V_{\text{super}} = \sum_{\text{routes}} \frac{V(d-B_1)V(B_n-a)}{\Delta E(d-B_1)} \prod_{j=1}^{n-1} \frac{V(B_{j+1}-B_j)}{\Delta E(d-B_{j+1})} \quad (4)$$

Here $V(d-B_1)$, $V(B_{j+1}-B_j)$, and $V(B_n-a)$ are the nearest-neighbor matrix elements, and $\Delta E(d-B_j)$ are the energy gaps. The sum in eq 4 is taken over all of the coupling routes (when a single route may dominate). Equation 4 is often approximated in an exponential donor–acceptor distance (R) dependence

$$V_{\text{super}} = V(d-B_1) \exp(-\beta R/2) \quad (5)$$

where

$$\beta = (2/R_0) \sum_{j=1}^{n-1} \ln[V(B_{j+1}-B_j)/\Delta E(d-B_{j+1})] + \ln[V(B_n-a)/\Delta E(d-B_1)] \quad (5a)$$

and R_0 is the (average) nearest neighbor spacing in the bridge. Equations 3 and 5 result in the superexchange rate

$$k_{\text{super}} = (2\pi/\hbar) |V(d-B_1)|^2 \exp(-\beta R) F \quad (6)$$

in analogy with the Robinson relation, eq 2b.

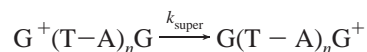
We note in passing that the perturbative expression, eqs 3 and 4, for the superexchange rate implies that the initial electronic wave function involves the mixing of the (zero-order) bridge states into the donor state. On the other hand, the off-resonance mixing of the charged donor states into the bridge states is not involved in the dynamics.

The superexchange mechanism was widely applied for chemical systems, consisting of rigid or semirigid, covalently bridged, donor–acceptor supramolecules.^{14–19} The fingerprint of the electronic superexchange interaction constitutes the well-known exponential distance dependence of the ET rate,^{14–18,23} eq 6. Nevertheless, such an analysis contains the hidden assumption that the nuclear Franck–Condon factor, which contains the R dependent medium reorganization energy, is approximately distance independent.^{24,25} Such an assumption is valid for the activationless and/or inverted region but may fail in the “normal” region for ET.

The superexchange interactions are ubiquitous for ET in biological systems, e.g., globular proteins, where long-range ET occurs, being mediated by the off-resonance superexchange electronic coupling with the polypeptide backbone.²⁶ Some superexchange mechanisms are operative for ET in membrane proteins, e.g., the photosynthetic reaction centers (RCs) of bacteria and plants.^{19–22} The major path of the primary charge separation in wild-type bacterial RCs involves a sequential ET from the bacteriochlorophyll dimer (P), via the accessory bacteriochlorophyll (B), to the bacteriopheophytin (H), because of resonance P^*-B interaction.^{19,27} Nevertheless, the superexchange mechanism is operative in a fraction of the wild-type RCs, because of inhomogeneous energetic broadening, which results in an off-resonance P^*-B interaction^{19,22} and dominates in some chemically engineered RCs.²⁸ Superexchange interactions also dominate the quinone (Q) reduction process in the photosynthetic RC, where Trp-M252 mediates ET between H⁻ and Q, contributing in a specific way to the electronic coupling through the protein.²⁹

Another class of charge transfer and transport in biological systems pertains to DNA, whose electronic properties are of fundamental interest in the context of radiation damage and repair,³⁰ as well as in the novel areas of electronic-nuclear response, dynamics and function of nanostructures, and molecular electronic systems.^{31,32} The majority of the experimental information on charge transport in DNA involves positive charge (hole) migration, i.e., the propagation of the radical cation along the duplex.^{33–44} Energetic data and computational results^{23,45–48} show that G nucleobases act as “resting”, lowest energy, states for holes in DNA duplexes, in accord with the experimental data.^{33–41} The interrogation of individual elementary steps of charge injection, trapping, hopping, and recombination, and their lifetimes in (intercolated, substituted or capped) DNA was accomplished by utilizing the arsenal of microsecond to femtosecond time-resolved methods.^{37–39,49–51} Concurrently, experimental evidence for long-range hole transport over distance scales of 40–200 Å emerged from the experiments of Barton,^{35,36} Schuster,^{33,43,44} and Giese^{34,40–42,52} on guanine relative chemical yield data.

The compound mechanism of hole transport in a DNA duplex $dG_1(T-A)_n G_2 \dots G_N$ containing N guanine nucleobases separated by $(T-A)_n$ bridges between a donor (d) and an acceptor (trap) t, e.g., G, GG, or GGG, involves several steps: (i) hole injection from d to the proximal G_1 , (ii) a sequence of reverse hole hopping processes between adjacent guanines, i.e., G_j and $G_{j\pm 1}$ within the bridge, and (iii) hole trapping/detrapping between G_N and t. The individual hole hopping processes (ii) between G_j and $G_{j\pm 1}$, which are separated by moderately short $(T-A)_n$ bridges ($n \lesssim 3$), correspond to unistep superexchange mediated hopping.^{23,51–60,31–42} Each hopping step is induced by superexchange, off-resonance, electronic coupling between G_j and $G_{j\pm 1}$ via the $(T-A)_n$ subbridges. The hole states of the $(T-A)_n$ ($n \lesssim 3$) subbridge are virtual and do not constitute a genuine chemical intermediate. The kinetic scheme for the individual unistep superexchange hopping rate is



where k_{super} is given by eqs 3 and 4. This physical picture of unistep hole superexchange hopping between guanines separated by “short” $(T-A)_n$ ($n \leq 3-4$) subbridges was proposed and analyzed in detail^{53–59} to account for the experimental yield data of Giese et al.^{40–42} and of Saito et al.⁶¹ In this paper, we utilize the intrastrand and interstrand hole transfer matrix

elements^{62,63} to evaluate the superexchange electronic couplings, which determine hole hopping within the framework of a quantum mechanical-kinetic model. We explore the compound hole hopping mechanism in DNA, which involves $G^+ \dots G$ superexchange mediation via “short” $(T-A)_n$ bridges. Previous studies of superexchange induced by intrastrand interactions^{23,53–58} will be extended for $G^+ \dots G$ superexchange mediated interstrand coupling via short bridges. The time-resolved experiments of Barton et al.⁵¹ for hole transport in the presence of a site-specifically bound methyltransferase $M \cdot HhaIQ237W$ mutant revealed that the observed hole transport rate ($k = 3–5 \times 10^6 \text{ s}^{-1}$) between the initial and the terminal G is higher by several orders of magnitude than that inferred from sequential intrastrand $G \dots G$ hopping steps for superexchange in this system.⁵¹ We shall show that these experimental results⁵¹ are compatible with a sequential multistep interstrand hopping mechanism. Of considerable interest is the issue of the range of the $(T-A)_n$ bridge length for the applicability of the superexchange mechanism in DNA, i.e., when does the superexchange exponential distance dependent mechanism break down? For “long” $(T-A)_n$ ($n > 3$) bridges, the $G^+(T-A)_nG$ unistep superexchange hopping is replaced by the (parallel) thermally induced hopping (TIH) mechanism, which involves thermally induced endothermic G^+A hole excitation to A followed by multistep hole hopping within the $(A)_n$ chain.^{36,52,54,60,64} The crossover between superexchange and TIH in DNA occurs at $n_c = 3–4$.^{52,60,64} The interesting experimental chemical yield data of Schuster et al.⁶⁵ for hole transport between seven GG groups, which are separated by $(T-A)_n$ ($n = 2–5$) bridges, were presented as evidence for the breakdown of the superexchange mechanism.⁶⁵ These data will be interpreted in terms of superexchange for the “short” $n = 2$ bridge, superexchange-TIH crossover for $n \cong 3$, and TIH transport for “long” $n = 3–5$ bridges.

II. Intrastrand and Interstrand Superexchange Coupling

The electronic coupling matrix elements for hole transfer between nearest-neighbor nucleobases^{62,63} can be utilized for the estimates of the superexchange interaction. Although complete theoretical estimates of hole transfer matrix elements in DNA duplexes containing up to three Watson–Crick pairs were carried out by us,⁶³ the perturbative superexchange expression, eq 4, is adequate for reliable semiempirical estimates of the electronic interactions, which rest on the use of pair electronic matrix elements, together with empirical energy gaps.⁶³ The pair electronic coupling matrix elements for both intrastrand and interstrand coupling (Figure 1) depend on the nature of the nucleobases. Hole transport between guanine hole “resting” states, separated by other nucleobases $B_1B_2 \dots$, can occur by superexchange-induced hopping $G^+B_1B_2 \dots G \rightarrow GB_1B_2 \dots G^+$ (where $B_1, B_2, \dots \neq G$), portrayed in Figure 1 parts a–d or, alternatively, by nearest-neighbor interstrand or intrastrand direct hopping $G^+G \rightarrow GG^+$ (Figure 1e). The bridge specificity is dominated by the pair electronic matrix elements, which determine the electronic coupling V and the rate $k \propto |V|^2$ for $G^+ \dots G$ direct hopping or superexchange. The intrastrand coupling matrix elements (for idealized structures) fall in the range 0.03–0.16 eV, being in most cases larger than the interstrand coupling matrix elements between the corresponding nucleobases, which fall in the range 0.001–0.06 eV. The only exception involves the interstrand A–A coupling, which is comparable to and even somewhat larger than, the intrastrand coupling. This exceptional case of A–A couplings,^{62,63} which is of considerable interest for the mechanism of TIH,^{60,64} demonstrates that the many-electron pair electronic couplings

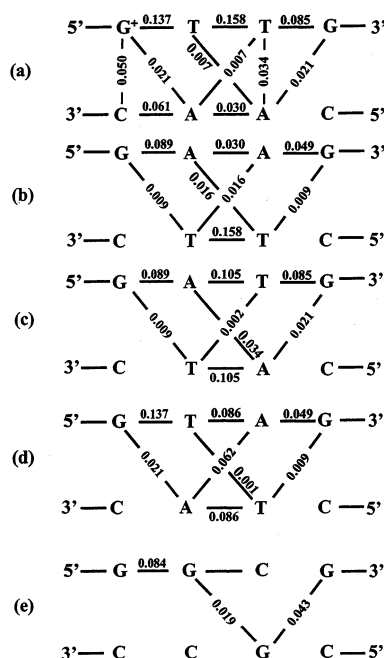


Figure 1. Electronic coupling matrix element (in eV) units between nearest-neighbor nucleobases in DNA duplexes (from refs 62 and 63). Both intrastrand and interstrand electronic couplings are presented. Note the directional asymmetry of the pair electronic interactions. The intrastrand interactions are the largest, whereas the G–T, T–T, and A–T interstrand interactions are considerably lower. A notable exception is the A–A intrastrand and interstrand electronic couplings, which are close and large, promoting TIH via long $(A)_n$ chains (refs 60 and 64). The interstrand $G \dots G$ electronic coupling, although lower than the corresponding intrastrand pair interaction, is sufficiently large to warrant effective interstrand hole hopping.

between nucleobases exhibit a marked angular dependence. Finally, we note that regarding nearest-neighbor $G \dots G$ coupling, which promotes direct hole hopping between guanines, both the intrastrand and the interstrand coupling are sufficiently large and both provide a route for hole hopping, although the interstrand coupling is lower (Figure 1e).

Two characteristics of the perturbative calculations of the superexchange interactions should be noted. First, minimization of the number of pair interactions which contribute to the superexchange electronic interaction, eq 4, is essential. For example, we note that although the matrix elements between nucleobases in the Watson–Crick pair are quite large (Figure 1a), the contribution of the route involving the Watson–Crick pair interaction will be smaller than that of an intrastrand (or interstrand) contribution which involves a smaller number of $V(B_1-B_2)/\Delta E$ terms. Second, the choice of a dominating single route for the superexchange contribution is often possible in DNA. A cursory examination of the pair matrix elements, which determine the intrastrand $G^+ \dots G$ superexchange interactions in some typical cases (Figure 1), allows us to choose a single dominating route for these interactions, eq 4. Of course, in some other cases, as for interstrand couplings (section III), several superexchange routes have to be incorporated in the calculation of V_{super} .

For the $G^+ \dots G$ superexchange coupling via $(T-A)_n$ bridges (Figure 1 parts a and b), the intrastrand superexchange electronic matrix elements, eq 4, were calculated for a single dominating route. In these calculations, we employed the pair matrix elements (Figure 1), together with the empirical energy gaps $\Delta E(G-A) = 0.22 \pm 0.05$,^{60,64} $\Delta E(G-T) = 0.6$,^{23,60} and $\Delta E(G-C) = 0.6 \text{ eV}$.²³ The $(T-A)_n$ bridge length dependence of $|V_{\text{super}}|^2$ (Figure 2) is exponential, as expected. Expressing $|V_{\text{super}}|^2 \propto$

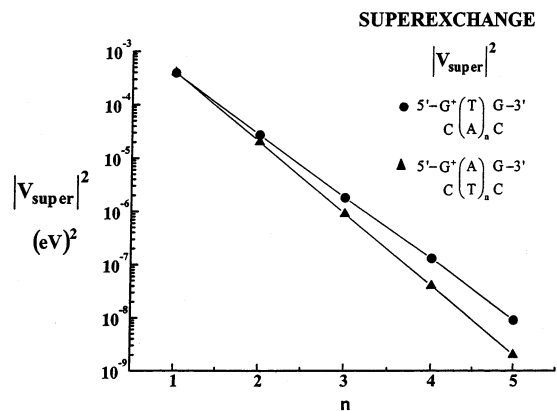
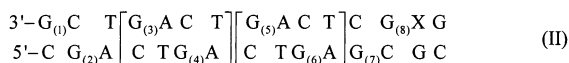
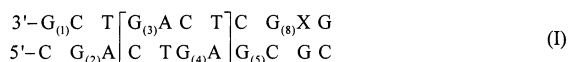


Figure 2. Exponential distance dependence of the superexchange intrastrand interactions $|V_{\text{super}}|^2$ for the two duplexes (—●— and —▲—) marked on the figure. $|V_{\text{super}}|^2$ data were calculated from the matrix elements of Figure 1 and semiempirical energy gaps (see text), with a single dominating superexchange route.

$\exp(-\beta R)$, we obtain $\beta = 0.78 \text{ \AA}^{-1}$ for the $G^+(T)_nG$ duplex and $\beta = 0.92 \text{ \AA}^{-1}$ for the $G^+(A)_nG$ duplex, exhibiting a weak (15%) bridge specificity. A heuristic common analysis^{23,37–39,40–42} of the superexchange rates in DNA sets $k_{\text{super}} = (2\pi/\hbar)|V_{\text{super}}|^2 F \propto \exp(-\beta R)$, neglecting the R dependence of F . These β values obtained from our theoretical scheme for $|V_{\text{super}}|^2$ are in accord with the experimental data $\beta = 0.6–0.8 \text{ \AA}^{-1}$ obtained from time-resolved studies of rates for hole injection^{37–39} and chemical yield data of hole trapping^{34,40–42} in DNA. Despite this apparently good agreement between the β values obtained from our calculations of $|V_{\text{super}}|^2$ and the experimental k_{super} data, a further exploration of the distance dependence of F (ref 25) will be of considerable interest.

III. Superexchange Mediated Interstrand Sequential Hole Transport

We have demonstrated that intrastrand electronic coupling can dominate the superexchange intrastrand interaction between adjacent G nucleobases. In some cases the interstrand superexchange or direct coupling can be sufficiently strong to warrant interstrand $G\dots G$ hole hopping. Recent experimental data of Barton et al.⁵¹ provide evidence for sequential interstrand hole transport. Time-resolved hole transport was experimentally explored in DNA assemblies in the presence of a site-specifically bound methyltransferase HhaIQ237W mutant in a series of duplexes:



where X is the mutant binding site which inserts a tryptophan side chain acting as a hole sink, whereas the G nucleobases are labeled consecutively according to their ordering in duplex (II). As observed by Barton et al.,⁵¹ the hole transfer rates from $G_{(1)}$ to X, $k \approx 3 \times 10^6 - 5 \times 10^6 \text{ s}^{-1}$, are close in the longer duplex (II) and in the shorter duplex (I). As noted by Barton et al.,⁵¹ their experimental rates for (I) and (II) cannot be reconciled with the intrastrand, sequential, superexchange hopping mechanism, i.e., (for duplex II)

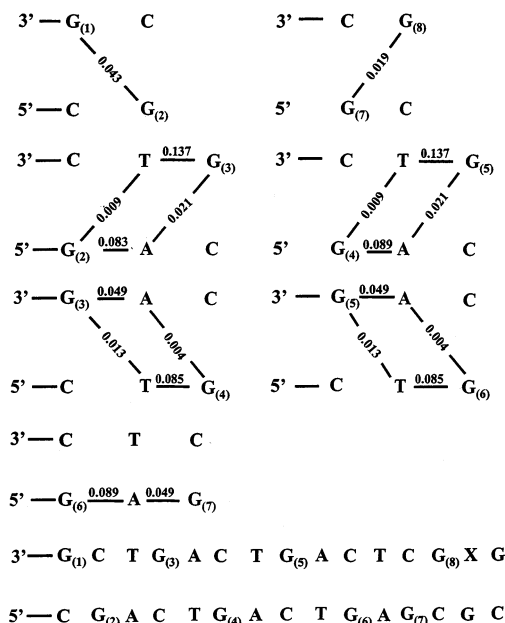
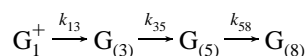


Figure 3. Electronic matrix elements (in eV; from refs 62 and 63) for the elementary interstrand and intrastrand $G^+\dots G$ superexchange mediated hopping (via a single nucleobase) and the direct hole hopping steps in duplex (II), which is presented on the bottom of the figure (adopted from ref 51). Note that, although the intrastrand superexchange coupling involves a single dominating route, the interstrand superexchange couplings involve two effective routes.

as the slowest rate determining intrastrand rate k_{58} involves $G_{(5)}^+ACTCG_{(8)}$ superexchange mediation over four nucleobases, rendering the $|V_{\text{super}}|^2$ couplings and the unistep rate to be very low. Using the time-resolved data of Lewis et al.,^{37–39} $k_{\text{super}}^{(L)}(G^+AG \rightarrow GAG^+) = 5 \times 10^7 \text{ s}^{-1}$, the corresponding intrastrand superexchange electronic coupling calculated from the pair matrix elements^{62,63} is $|V_{\text{super}}^{(L)}| = 1.7 \times 10^{-2} \text{ eV}$, whereas the $G_{(5)}-G_{(8)}$ intrastrand superexchange coupling is calculated as $|V_{\text{super}}^{5-8}| = 3.7 \times 10^{-5} \text{ eV}$ from the pair coupling matrix elements and semiempirical energy gaps (section II). Thus, $k_{58} = (|V_{\text{super}}^{5-8}|^2/|V_{\text{super}}^{(L)}|^2)k_{\text{super}}^{(L)}$ results in $k_{58} = 2.4 \times 10^2 \text{ s}^{-1}$, which is lower by 4 orders of magnitude than the experimental value of k . Accordingly, intrastrand superexchange is indeed excluded.⁵¹

We proposed⁶⁰ that the experimental results of Barton et al.⁵¹ are compatible with composite, multistep, sequential $G^+\dots G$ interstrand and intrastrand hole hopping. For duplex (II), the individual hopping $G^+\dots G$ steps fall into three categories: (i) interstrand superexchange mediated by a single nucleobase, (ii) intrastrand superexchange mediated by a single nucleobase, and (iii) direct interstrand coupling. The electronic couplings $|V^{i-j}|$ for the superexchange mechanism between $G_{(i)}^+$ and $G_{(j)}$ (categories i and ii) were evaluated according to eq 4, using the pair matrix elements,^{62,63} which are presented in Figure 3, and the empirical energy gaps (section II). We also present in Figure 3 the $G_{(i)}^+\dots G_{(j)}$ matrix elements for direct interstrand coupling (category iii). The relevant intrastrand and interstrand coupling matrix elements exhibit directional asymmetry in the $5'-3'$ and $3'-5'$ directions. Although the intrastrand superexchange induced hopping is well documented both experimentally and theoretically, the interstrand mediation of hopping manifested by the results of Barton et al.⁵¹ is new and interesting, revealing the following features. First, we shall establish that the interstrand superexchange couplings via a single mediating nucleobase, although lower than a corresponding intrastrand superexchange (via a single nucleobase), are sufficiently strong to

warrant effective hole hopping between adjacent G nucleobases on different strands of the duplex and zigzagging between the strands. Second, the interstrand superexchange couplings (2) \leftrightarrow (3), (4) \leftrightarrow (5), (3) \leftrightarrow (4), and (5) \leftrightarrow (6) involve two routes with comparable contributions (Figure 3). This pattern of interstrand superexchange coupling is distinct from the intrastrand superexchange, e.g., (6) \leftrightarrow (7), which involves a single dominant route (Figure 3). The contributions of the different routes to the interstrand superexchange coupling were arbitrarily taken with the same sign, following our previous discussion of the phase problem for the coupling routes in DNA.⁶³

The relevant electronic couplings for interstrand/intrastrand superexchange via single bridges and for direct interstrand exchange are given by

$$\begin{aligned} G_{(1)}^+ &\xrightarrow{k_{12}} G_{(2)} & |V^{1-2}| &= 4.3 \times 10^{-2} \text{ eV} \\ G_{(2)}^+ &\xrightarrow{k_{23}} G_{(3)} \text{ and } G_{(4)}^+ \xrightarrow{k_{45}} G_{(5)} & |V^{2-3}| &= |V^{4-5}| = 9.0 \times 10^{-3} \text{ eV} \\ G_{(3)}^+ &\xrightarrow{k_{34}} G_{(4)} \text{ and } G_{(5)}^+ \xrightarrow{k_{56}} G_{(6)} & |V^{3-4}| &= |V^{5-6}| = 2.6 \times 10^{-3} \text{ eV} \\ G_{(6)}^+ &\xrightarrow{k_{67}} G_{(7)} & |V^{6-7}| &= 1.7 \times 10^{-2} \text{ eV} \\ G_{(7)}^+ &\xrightarrow{k_{78}} G_{(8)} & |V^{7-8}| &= 1.9 \times 10^{-2} \text{ eV} \end{aligned} \quad (7)$$

As $k_{ij} \propto |V^{i-j}|^2 F$ and the Franck–Condon factors F for all of the nearly symmetric ($\Delta G = 0$) reactions are approximately equal, we can estimate the rate from the experimental results of Lewis et al.^{37–39} $k_{67} = k_{\text{super}}^{(L)}(G^+AG \rightarrow GAG^+) = 5 \times 10^7 \text{ s}^{-1}$. Scaling the other rates by the ratios of the corresponding $|V|^2$ values, we get $k_{ij} = (|V^{i-j}|^2/|V^{6-7}|^2)5 \times 10^7 \text{ s}^{-1}$. We thus obtain $k_{12} = 3.2 \times 10^8 \text{ s}^{-1}$, $k_{23} = k_{45} = 1.4 \times 10^7 \text{ s}^{-1}$, $k_{34} = k_{56} = 1.2 \times 10^6 \text{ s}^{-1}$, $k_{67} = 5 \times 10^7 \text{ s}^{-1}$ (fit from Lewis' data³⁸), and $k_{78} = 6.2 \times 10^7 \text{ s}^{-1}$. We thus infer that the direct interstrand hole transfer rates k_{12} and k_{78} are the largest, being higher by numerical factors of 1.2–6 than the rate k_{67} for the intrastrand superexchange. Regarding intrastrand and interstrand $G^+ \dots G$ superexchange mediated rates, the interstrand superexchange coupling is sufficiently strong to induce effective hole hopping. Nevertheless, the superexchange interstrand hopping rates $k_{23} = k_{45}$ and $k_{34} = k_{56}$ are the lowest among all of the relevant rates. The rates of the slowest reactions in the sequential kinetic scheme are $k_{34} = k_{56} = 1.2 \times 10^6 \text{ s}^{-1}$, which constitute the rate determining steps in duplex (II). Accordingly, the radical oxidation rate k is expected to be given by these rate-determining rates. The composite, sequential interstrand/intrastrand hopping mechanism in duplexes (II) and (I) reveals the following features:

(1) It accounts well for the time-resolved data of Barton et al.,⁵¹ with the calculated rate determining rates $k_{34} = k_{56} = 1.2 \times 10^6 \text{ s}^{-1}$ being in reasonable agreement with the experimental result⁵¹ $k = 3 \times 10^6 - 5 \times 10^6 \text{ s}^{-1}$.

(2) This sequential interstrand mechanism implies a weak duplex size dependence of the rate k for sequences (I) and (II), where the rate determining step is identical. This conclusion is in accord with the experimental results.⁵¹

(3) Although the interstrand hole crossing between the two strands of the duplex is often less effective than the intrastrand hopping, the “penalty factor”⁵¹ for interstrand crossing is not very small and is bridge specific. The calculations of the individual rates given above result in a “penalty factor” (i.e., the ratio $p = k_{ij}/k_{67}$) of $p = 0.024$ for $G_{(3)}^+ - G_{(4)}$ and $G_{(5)}^+ - G_{(6)}$, whereas $p = 0.3$ for $G_{(2)}^+ - G_{(3)}$ and $G_{(4)}^+ - G_{(5)}$ superexchange coupling. For the direct interstrand $G_{(1)}^+ - G_{(2)}$ and $G_{(7)}^+ - G_{(8)}$ couplings, $p > 1$ and no penalty exists.

The most important conclusion emerging from our analysis is that the multistep, sequential interstrand/intrastrand hole hopping via short (T–A) bridges (with one superexchange mediating nucleobase) can induce long-range charge transport over a distance scale of 50 Å in DNA, as experimentally demonstrated by Barton et al.⁵¹ Of course, the realization of this mechanism requires the chemical engineering of the DNA duplex, with the G nucleobases being separated by “short” (T–A)_n bridges.

IV. Intrastrand Hole Hopping Mediated by (A–T)_n Base Pairs and the Breakdown of the Superexchange Mechanism

Extensive experimental and theoretical studies have revealed that intrastrand hole (radical cations) migration occurs through DNA by a series of short-range hops between adjacent G nucleobases, which are separated by a bridge of (T–A)_n base pairs.^{23,33–45,53–59} Long-distance hole transport via G nucleobases separated by two (T–A)₂ Watson–Crick pairs in the duplexes GTTGTG...TTGGG over a distance scale of 10–40 Å were experimentally studied by Giese et al.^{40–42} and were analyzed^{53–60} in terms of a sequence of G^+TTG superexchange hopping steps. The intrastrand hole migration through the G bases was interrogated by the relative chemical yields for the reaction of G^+ with water (reaction rate k_r). The analysis of the long-range transport data of Giese et al.^{40–43} resulted in^{53–55} $k(2)/k_r = 12.5$, where $k(2)$ is the hopping rate between adjacent G bases in $G^+(T-A)_2G$. A central question pertains to the range of applicability of the superexchange mechanism, i.e., whether increasing the (T–A)_n bridge length will manifest an exponential decrease of the $G^+(T-A)_nG$ hopping rate, as appropriate for superexchange. A negative answer to this question was already provided by the relative chemical yield (R) data of Barton et al.³⁶ in the duplex $GG^+(A)_nGG$ ($n = 4-10$), where R exhibits a weak bridge length dependence, and by the hole trapping data of Giese et al.⁵² in the duplex $G^+(T)_nGGG$ ($n = 1-16$), where R manifests an exponential (superexchange) bridge length (n) dependence for $n = 1-3$, whereas for $n = 4-16$ a weak bridge length dependence, contradicting the superexchange mechanism, is manifested. The breakdown of the superexchange mechanism for longer (T–A)_n bridges, i.e., $n \gtrsim 3-4$, was attributed^{36,52,60,64} to the onset of the TIH mechanism via (A)_n chains. The TIH involves endothermic hole activation from G^+ to A followed by hole hopping among A bases and exhibits a weak (algebraic) $G^+ \dots G$ distance dependence.

The “transition” between superexchange ($n < n_x$) and TIH ($n > n_x$) in DNA is expected to occur^{36,60,64} at $n \approx n_x \approx 3-4$. Sartor, Boone, and Schuster⁶⁵ presented an experimental study of hole transport through seven GG pairs within the 3'–5' strand of the DNA duplex presented in Figure 4, where the GG groups are separated by (T–A)_n ($n = 2-5$) Watson–Crick pairs. The exploration of long-range hole transport between the groups $(GG)_1^+ - (GG)_N$ ($N = 2-7$), i.e., over a distance scale of 82 Å for $n = 2$ and 112 Å for $n = 5$, with changing the (T–A)_n bridge length ($n = 2-5$), provides a critical scrutiny for the superexchange mechanism. Schuster et al.⁶⁵ qualitatively inferred from their experimental results that the yield data are incompatible with an exponential bridge length dependence of the yield, pointing toward the failure of the superexchange mechanism over the entire range $n = 2-5$. We shall show that these experimental yield data of Schuster et al.⁶⁵ (Figure 4) are compatible with a crossover from superexchange at $n = 2$ to TIH at a higher bridge size.

We proceed with an analysis of the experimental data of Schuster et al.⁶⁵ for the shortest bridge $n = 2$, where superex-

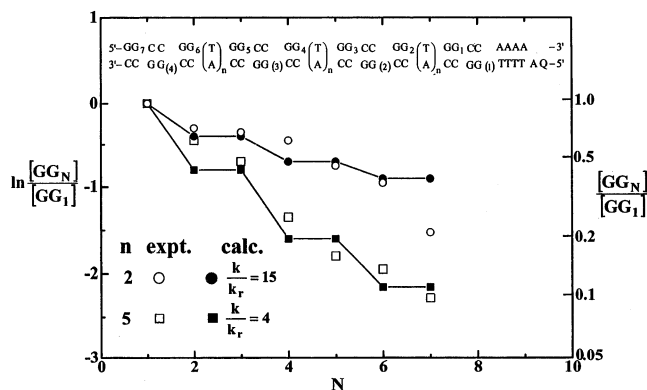
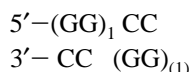
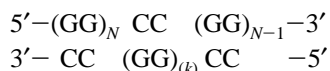


Figure 4. Kinetic analysis of the experimental chemical yield data of Sartor, Boone, and Schuster (ref 65) for injection from anthraquinone (AQ) to $GG_{(1)}$ and GG_1 followed by hole transport in the DNA duplex shown on the figure. The experimental normalized relative yields (ref 65) for GG_N/GG_1 ($N = 1-7$) of the guanine doublets across the 3'-5' direction of the DNA duplex (marked on the top of the figure) are given for two bridge lengths (\circ) $n = 2$ and (\square) $n = 5$. The kinetic analysis is based on the assumption of thermal equilibration between nearest-neighbor GG hole states. The solid lines represent the results for the kinetic scheme, eq 8, given for (\bullet) $n = 2$ and for (\blacksquare) $n = 5$. One-parameter fits of the experimental data are given by $k/k_r = 15$ for $n = 2$ and $k/k_r = 4$ for $n = 5$, where k is the $GG_N^+(T)_nGG_{N+1}$ hopping rate and k_r is the reaction rate of GG^+ with water.

change mediation is expected to occur. The single-strand hole hopping between the adjacent $(GG)_N$ ($N = 1-7$) doublets (Figure 4) involves two types of elementary steps: (i) intrastrand hole hopping $(GG)_N^+(T-A)_2(GG)_{N+1}$ ($N = 1-7$) between adjacent $(GG)_N$ pairs across the single 3' - 5' strand and (ii) interstrand hole hopping between nearest-neighbor GG groups, i.e., in the pairs of doublets



and in the triplets of doublets



where ($N = 2, (k) = 2$; $N = 4, (k) = 3$; and $N = 6, (k) = 4$). Both the nearest-neighbor G-G intrastrand coupling $|V(G|G)|^2 = 7.1 \times 10^{-3} \text{ eV}^2$, the interstrand pair couplings $|V(G/G)|^2 = 3.6 \times 10^{-4} \text{ eV}^2$ (in the 5'-5' direction), and $|V(G/G)|^2 = 1.8 \times 10^{-3} \text{ eV}^2$ (in the 3'-3' direction; Figure 1e) are considerably larger (by more than an order of magnitude) than the superexchange coupling $|V(GTTG)|^2 = 2.6 \times 10^{-5} \text{ eV}^2$. We thus expect that both the intrastrand and interstrand nearest-neighbor G^+G hopping rates are faster by 1-2 orders of magnitude than the G^+TTG superexchange hopping. Accordingly, thermal equilibrium prevails within each doublet, between the pair doublets $N = 1$ and $k = (1)$, and within the triplets of doublets $N = 2$ and 3, $k = (2)$; $N = 4$ and 5, $k = (3)$; $N = 6$ and 7, $k = (4)$. On the basis of our energetic data,^{48,55} we infer that the energies of $(T-A)G^+G(T-A)$ and $(T-A)GG^+(T-A)$ duplexes are nearly equal. The thermal equilibration implies an equal hole population probability among the individual G components of the pair of doublets or of the triplets of doublets mentioned above. The kinetic scheme within this framework for the thermalized population probabilities F_N ($N = 1, \dots, 7$) with

$$\begin{aligned} F_1 &= [GG_1] = [GG_{(1)}], & F_2 &= [GG_2] = [GG_{(2)}] = [GG_3] \\ F_3 &= [GG_4] = [GG_{(3)}] = [GG_5], & F_4 &= [GG_6] = [GG_{(4)}] = [GG_7] \end{aligned}$$

is given by

$$\begin{aligned} dF_1/dt &= -(k(n) + 2k_r)F_1 + k(n)F_2 \\ dF_2/dt &= k(n)F_1 - (2k(n) + 3k_r)F_2 + k(n)F_3 \\ dF_3/dt &= k(n)F_2 - (3k_r + 2k(n))F_3 + k(n)F_4 \\ dF_4/dt &= k(n)F_3 - (3k_r + k(n))F_4 \end{aligned} \quad (8)$$

where $k(n)$ [$n = 2$] is the hole hopping rate between G_N and G_{N+1} across the $(T-A)_n$ bridge, i.e., $GG_N^+ \xrightleftharpoons{k(n)} (GG)_{N+1}$. k_r is the rate of the reaction of $(GG)^+$ with water.^{33-36,40-44} No evidence is available on the site specificity of the reaction of G with water. A single parameter fit (Figure 4) of the chemical yield rate for $n = 2$ works reasonably well with $k(2)/k_r = 15$. The experimental data, within their experimental accuracy, are in accord with the assumption of thermal equilibrium which gives "steps" in the GG_N vs N dependence (Figure 4). The ratio $k(2)/k_r = 15$ of the rates for the hopping over the $n = 2$ bridge and the reaction of G^+ with water is in excellent agreement with the analysis⁵³⁻⁵⁵ of the independent experimental data⁴⁰⁻⁴² for the rates of charge hopping/water reaction in the $G^+TTG\dots$ duplex, which gives $k(2)/k_r = 10-12$. It is gratifying that good agreement is obtained between k/k_r data from two laboratories.^{40-42,65}

Moving to the longest $(T-A)_5$ bridge studied by Schuster et al.,⁶⁵ the heuristic analysis based on the concept of thermal equilibration, eq 8, results in a reasonable fit of the experimental data with $k(5)/k_r = 4$ (Figure 4). For lower values of $n = 3$ and 4, we used similar fits, estimating $k(3)/k_r = 4-5$ for $n = 3$ and $k(4)/k_r = 4-5$ for $n = 4$. The spread of the experimental data in all cases is substantial, as is apparent from Figure 4. Nevertheless, from Schuster's experiments⁶⁵ and our analysis of hole transport in their duplex (Figure 4), we conclude that:

(1) For the short $n = 2$ bridge size, the superexchange mechanism prevails.

(2) The "transition" from superexchange to TIH is exhibited at $n = n_x \approx 3$. The superexchange-TIH crossover is in accord with the quantum mechanical kinetic theoretical estimate $n_x = 3-4$.

(3) At finite temperatures, the superexchange and TIH channels occur in parallel. However, for short bridges ($n = 1$ and 2), the superexchange mechanism dominates. On the basis of detailed analytical and numerical analyses,^{60,64} the contribution of the parallel TIH mechanism is negligible for the short $n = 1$ and 2 bridge (i.e., less than 5% for $n = 2$). On the other hand, for long bridges ($n > 4$) the TIH channel dominates over the parallel superexchange channel.

(4) In the TIH domain, i.e., for $n = 3, 4, \text{ and } 5$, the $G^+\dots G$ hopping rate k exhibits a weak bridge size dependence, which predicts a weak (algebraic) n dependence of the $G^+\dots G$ TIH rates, which are expected to be given by⁶⁴ $k = 1/\{1/k_1 + [(n-1)/k_{A-A}] \exp(\Delta/k_B T)\}$, where k_1 is the G^+A endothermic hole injection rate, Δ is the energy gap for the injection, and k_{A-A} is the hole hopping rate between adjacent A bases.

Schuster's experimental data⁶⁵ for the superexchange-TIH crossover at $n_x \approx 3$ concur with the experiments of Giese et al.⁵² for hole trapping in the $G^+(T-A)_nGGG$ ($n = 1-16$) duplex, which gave $n_x = 3$. The weak bridge size dependence of $k(n)/k_r$ inferred from Schuster's data for $n = 3-5$ is consistent with the relative chemical yield data of Barton et al. for the $GG^+(A)_nGG$ ($n = 4-10$) duplex³⁶ and of Giese et al. for the $G^+(T-A)_nGGG$ ($n = 4-16$) duplex.⁵² It is surprising that in the experimental data of Schuster et al.⁶⁵ the reduction of the

GG⁺...GG superexchange rate between $n = 2$ and 3 is $r = k(3)/k(2) = 0.25$, which is lower by a numerical factor of 2–3 from the reduction factor of $r = \exp(-\beta R_0) \approx 0.1-0.07$ expected for superexchange coupling (Figure 2). To establish whether $k(2)$ and $k(3)$ indeed correspond to superexchange mediated hopping, it will be important to provide experimental data for the $n = 1$ (T–A) bridge in the duplex studied by Schuster et al.⁶⁵ (Figure 4). It should be borne in mind that in the foregoing quantum-mechanical-kinetic treatment we considered a rigid DNA structure, which is determined by the (average) nuclear equilibrium configuration. The nuclear configurational fluctuations of the DNA duplex, of the sugars and phosphates, of water, and of alkali cations may affect the energetics and the electronic couplings.^{66–69} These effects of configurational fluctuations, which are determined by the relative time scales of the electronic processes and of the fluctuations, were not incorporated in our analysis of superexchange hopping via short bridges and the breakdown of the superexchange mechanism, which is replaced by TIH for longer chains.

V. Epilogue

We established the range of the applicability of the superexchange mechanism for intrastrand (sections II and IV) and for interstrand (section III) hole hopping via “short” ($n = 1-3$) bridges in DNA. Superexchange provides a route for long-range charge transport between G sites separated by “short” bridges. The breakdown of the superexchange mechanism is of considerable interest, as the TIH mechanism for “long” bridges exhibits a weak (algebraic) bridge length dependence, in contrast with the exponential bridge length dependence for the superexchange, eq 4, via short bridges. Accordingly, the TIH provides a mechanism for very long-range charge transport in DNA.

It will be appropriate to conclude this exploration with a comment on the universality and system-specificity of the superexchange mechanism. The pioneering studies of George and Griffith,¹² Halpern and Orgel,¹³ and McConnel¹¹ on superexchange mediated electron transfer and of Robinson on superexchange induced triplet energy transfer^{4,5} laid the foundations for the universality of the superexchange mediation induced by off-resonance, short-range, pair electronic interactions for charge separation in large scale chemical systems, proteins, and DNA. The application and utilization and, even more interesting, the breakdown of the superexchange G⁺...G charge hopping mechanism in DNA explored herein, reveal a surprisingly low value of $n_x \approx 3$ for the superexchange–TIH “transition”. This modest bridge size for the breakdown of the superexchange mechanism in DNA is considerably lower than what is exhibited in other large chemical scale and biophysical systems, where superexchange prevails over a large domain of bridge sizes and no evidence for an alternative mechanism with increasing the bridge size was recorded^{14–21} or where n_x is considerably larger than in DNA.⁷⁰ The superexchange–TIH crossover is determined by the energetics and the electronic coupling. A recent analysis^{60,64} resulted in the following approximate simple relation for the crossover

$$n_x \approx 1 - \Delta/k_B T \ln r = 1 + \Delta/k_B T \beta R_0 \quad (9)$$

where Δ is the donor-bridge energy gap and $r = \exp(-\beta R_0)$ is the reduction factor upon the increase of the bridge by one unit. The superexchange–TIH crossover in DNA is quantitatively unique, as $\Delta = \Delta E(G^+A) = 0.22 \pm 0.05$ eV. The low G⁺A energy gap in DNA induces the “transition” (at room temperature) at a low value of n_x , which is in reasonable agreement

with Barton's,³⁶ Giese's,⁵² and Schuster's⁶⁵ experiments (section IV). Indeed, with $\Delta = 0.20$ eV, $\beta = 0.7 \text{ \AA}^{-1}$, $R_0 = 3.38$, and $T = 300$ K, we estimate from eq 9 the value of $n_x \approx 3.4$. This pattern for DNA is qualitatively different from other chemical and biophysical systems, where the parameter ($\Delta/k_B T$) is considerably larger and the superexchange mechanism is applicable over a large bridge size domain.

Acknowledgment. We are indebted to Professor G. A. Schuster for kindly communicating his paper to us prior to publication (ref 65) and for perceptive discussions, and to Professor J. K. Barton for stimulating discussions and exchange of information. This research was supported by the Deutsche Forschungsgemeinschaft (SFB 377), the Volkswagen Foundation, and the Fonds der Chemischen Industrie, Germany.

References and Notes

- Robinson, G. W.; McCarty, M. J. *J. Chem. Phys.* **1958**, *28*, 350.
- Robinson, G. W.; Frosch, R. P. *J. Chem. Phys.* **1962**, *37*, 1962.
- Colson, S. D.; Kopelman, R.; Robinson, G. W. *J. Chem. Phys.* **1967**, *47*, 27.
- Nieman, G. C.; Robinson, G. W. *J. Chem. Phys.* **1962**, *37*, 2150.
- Nieman, G. C.; Robinson, G. W. *J. Chem. Phys.* **1963**, *38*, 1326.
- Kopelman, R.; Monberg, E. M.; Ochs, F. W. *J. Chem. Phys.* **1977**, *19*, 413.
- Klafter, J.; Jortner, J. *J. Chem. Phys.* **1979**, *71*, 1961.
- Kramers, H. A. *Physica* **1934**, *1*, 182.
- Shull, C. G.; Stauser, W. A.; Wollan, E. O. *Phys. Rev.* **1951**, *83*, 333.
- Anderson, P. W. *Phys. Rev.* **1959**, *115*, 2.
- McConnel, H. M. *J. Chem. Phys.* **1961**, *35*, 508.
- George, M.; Griffith, J. S. In *The Enzymes 1*; Academic Press: New York, 1959; pp 347–392.
- Halpern, J.; Orgel, L. E. *Discuss. Faraday Soc.* **1960**, *29*, 32.
- Beratan, D. N. *J. Am. Chem. Soc.* **1986**, *108*, 4321.
- Heitele, H.; Michel-Beyerle, M. E. *J. Chem. Phys. Lett.* **1987**, *134*, 273.
- Warman, J. M.; De Haas, M. P.; Paddon-Row, M. N.; Cotsaris, E.; Hush, N. S.; Oevering, H.; Verhoeven, J. W. *Nature* **1986**, *320*, 615.
- Larsson, S.; Volosov, A. *J. Chem. Phys.* **1986**, *85*, 2548.
- Closs, G. L.; Miller, J. R. *Science* **1988**, *140*, 440.
- Bixon, M.; Jortner, J. *Adv. Chem. Phys.* **1999**, *106*, 35.
- Antennas and Reaction Centres of Photosynthetic Bacteria*; Michel-Beyerle, M. E., Ed.; Springer-Verlag: Berlin, 1985.
- The Photosynthetic Bacterial Reaction Center*; Breton, J.; Vermeglio, A., Eds.; Plenum Press: New York, 1988.
- Bixon, M.; Jortner, J.; Michel-Beyerle, M. E. *J. Chem. Phys.* **1995**, *103*, 389.
- Jortner, J.; Bixon, M.; Langenbacher, T.; Michel-Beyerle, M. E. *Proc. Natl. Acad. Sci. U.S.A.* **1998**, *95*, 12759.
- Brunschwig, B. S.; Ehrenson, S.; Sutin, N. *J. Am. Chem. Soc.* **1984**, *106*, 6858.
- Tavernier, H. L.; Fayer, M. D. *J. Phys. Chem. B* **2000**, *104*, 11541.
- Winkler, J. R. *Curr. Opin. Chem. Biol.* **2000**, *4*, 192.
- Spörlein, S.; Zinth, W.; Meyer, M.; Scheer, H.; Wachtveitl, J. *J. Chem. Phys. Lett.* **2000**, *322*, 454.
- Hartwick, B.; Bieser, B.; Langenbacher, T.; Müller, D.; Richter, M.; Orogodnik, A.; Scheer, H.; Michel-Beyerle, M. E. *Biophys. J.* **1998**, *72*, 8.
- Plato, M.; Michel-Beyerle, M. E.; Bixon, M.; Jortner, J. *FEBS Lett.* **1989**, *29*, 70.
- Heller, A. *Faraday Discuss.* **2000**, *116*, 1.
- Alivisatos, A. P.; Johnsson, K. P.; Wilson, T. E.; Loveth, C. J.; Bruchez, M. P.; Schultz, P. J. *Nature* **1996**, *382*, 609.
- Dekker, C.; Ratner, M. A. *Phys. Today* **2001**, *14*(8).
- Schuster, G. B. *Acc. Chem. Res.* **2000**, *33*, 253.
- Giese, B. *Acc. Chem. Res.* **2000**, *33*, 631.
- Núñez, M. E.; Hall, D. B.; Barton, J. K. *J. Chem. Biol.* **1999**, *6*, 85, 97.
- Williams, T. T.; Odon, D. T.; Barton, J. K.; *J. Am. Chem. Soc.* **2000**, *122*, 9048.
- Lewis, F. D.; Liu, X.; Liu, J.; Miller, S. E.; Hayes, R. T.; Wasielewski, M. R. *Nature* **2000**, *51*, 406.
- Lewis, F. D.; Liu, X.; Liu, J.; Hayes, R. T.; Wasielewski, M. R. *J. Am. Chem. Soc.* **2000**, *122*, 12037.
- Lewis, F. D.; Kalgutkar, R. S.; Wu, Y.; Liu, X.; Liu, J.; Hayes, R. T.; Miller, S. E.; Wasielewski, M. R. *J. Am. Chem. Soc.* **2000**, *122*, 12346.

- (40) Megger, E.; Michel-Beyerle, M. E.; Giese, B. *J. Am. Chem. Soc.* **1998**, *120*, 12950.
- (41) Giese, B.; Wessely, S.; Spormann, M.; Lindemann, U.; Meggers, E.; Michel-Beyerle, M. E. *Angew. Chem., Int. Ed. Engl.* **1999**, *38*, 996.
- (42) Giese, B.; Wessely, S. *Angew. Chem., Int. Ed.* **2000**, *39*, 3490.
- (43) Henderson, P. T.; Jones, D.; Hampkian, G.; Kan, Y.; Schuster, G. B. *Proc. Natl. Acad. Sci. U.S.A.* **1999**, *96*, 8353.
- (44) Sani, L.; Schuster, G. B. *J. Am. Chem. Soc.* **2000**, *122*, 11545.
- (45) Steenken, S.; Jovanovic, S. V. *J. Am. Chem. Soc.* **1997**, *119*, 617.
- (46) Hush, N. S.; Cheung, A. S. *Chem. Phys. Lett.* **1975**, *34*, 11.
- (47) Saito, J.; Nakamura, T.; Nakatani, K. *J. Am. Chem. Soc.* **2000**, *122*, 3001.
- (48) Voityuk, A. A.; Jortner, J.; Bixon, M.; Rösch, N. *Chem. Phys. Lett.* **2000**, *324*, 430.
- (49) Wan, C.; Fiebig, T.; Kelley, S. O.; Treadway, C. R.; Barton, J. K.; Zewail, A. H. *Proc. Natl. Acad. Sci. U.S.A.* **1999**, *96*, 6014.
- (50) Davis, W. B.; Naydenova, I.; Haselsberger, R.; Ogorodnik, A.; Giese, B.; Michel-Beyerle, M. E. *Angew. Chem., Int. Ed.* **2000**, *39*, 3649.
- (51) Wagenknecht, H.-A.; Rajski, S. R.; Pascally, M.; Stemp, E. D. A.; Barton, J. K. *J. Am. Chem. Soc.* **2001**, *123*, 4400.
- (52) Giese, B.; Amaudrut, J.; Kohler, A. K.; Spormann, M.; Wessely, S. *Nature* **2001**, *412*, 318.
- (53) Bixon, M.; Giese, B.; Wessely, S.; Langenbacher, T.; Michel-Beyerle, M. E.; Jortner, J. *Proc. Natl. Acad. Sci. U.S.A.* **1999**, *96*, 11713.
- (54) Bixon, M.; Jortner, J. *J. Phys. Chem. B* **2000**, *104*, 3906.
- (55) Bixon, M.; Jortner, J. *J. Phys. Chem.* **2001**, *105*, 2069.
- (56) Berlin, V. A.; Burin, A. L.; Ratner, M. *J. Phys. Chem. A* **2000**, *104*, 443.
- (57) Grozema, F. C.; Berlin, Y. A.; Siebbeles, L. D. A. *J. Am. Chem. Soc.* **2000**, *122*, 10903.
- (58) Grozema, F. C.; Berlin, Y. A.; Siebbeles, L. D. A. *Int. J. Quantum Chem.* **1999**, *75*, 1009.
- (59) Berlin, Y. A.; Burin, A. L.; Ratner, M. A. *J. Am. Chem. Soc.* **2001**, *123*, 260.
- (60) Bixon, M.; Jortner, J. *J. Am. Chem. Soc.* **2001**, *123*, 12556.
- (61) Nakatani, K.; Dohno, C.; Saito, I. *J. Am. Chem. Soc.* **1999**, *121*, 10854.
- (62) Voityuk, A. A.; Rösch, N.; Bixon, M.; Jortner, J. *J. Phys. Chem. B* **2000**, *104*, 9740.
- (63) Voityuk, A. A.; Jortner, J.; Bixon, M.; Rösch, N. *J. Chem. Phys.* **2001**, *114*, 5614.
- (64) Bixon, M.; Jortner, J. *Chem. Phys. Special Issue on Molecular Wires* **2001**, *105*, 11057.
- (65) Sartor, V.; Boone, E.; Schuster, G. B. *J. Phys. Chem. B* **2001**, in press.
- (66) Cheatham, T. E., III; Kollman, P. A. *Annu. Rev. Phys. Chem.* **2000**, *51*, 435.
- (67) Voityuk, A. A.; Siriwong, K.; Rösch, N. *Phys. Chem. Chem. Phys.* **2001**, *3*, 5421.
- (68) Barnett, R. N.; Cleveland, C. L.; Joy, A.; Landman, U.; Schuster, G. B. *Science* **2001**, *294*, 567.
- (69) Xie, Q.; Archontis, G.; Skourtis, S. S. *Chem. Phys. Lett.* **1999**, *312*, 237.
- (70) Isied, S. S.; Ogawa, M. Y.; Wishart, J. F. *Chem. Phys.* **1992**, *92*, 381.